Wurtzite-Type CoO Nanocrystals in Ultrathin ZnCoO Films

H. L. Meyerheim,[1] C. Tusche,[1] A. Ernst,[1] S. Ostanin,[1] I. V. Maznichenko,[2] K. Mohseni,[1] N. Jedrecy,[3] J. Zegenhagen,[4] J. Roy,[4] I. Mertig,[1,2] and J. Kirschner[1]

[1]*Max-Planck-Institut für Mikrostrukturphysik, Weinberg 2, D-06120 Halle, Germany*
[2]*Institut für Physik, Martin-Luther-Universität Halle-Wittenberg, D-06099 Halle, Germany*
[3]*Institut des Nano Sciences de Paris, Université P. et M. Curie-Paris 6 and CNRS-UMR7588, 75015 Paris, France*
[4]*ESRF, B.P. 220, F-38043 Grenoble Cedex, France*

(Received 7 December 2008; published 13 April 2009)

Surface x-ray diffraction experiments reveal that, in cobalt-doped ZnO films two to five monolayers thick, Wurtzite-type CoO nanocrystals are coherently embedded within a hexagonal boron-nitride-(*h*-BN)-type ZnO matrix, supporting the model of a phase separation. First-principles calculations confirm that, in contrast with ZnO, the formation of *h*-BN-type CoO is unfavorable in the ultrathin film limit. Our results are important for understanding magnetic properties of transition metal-doped semiconductors in general.

DOI: 10.1103/PhysRevLett.102.156102 PACS numbers: 68.47.Gh, 61.05.cp, 75.75.+a

Almost a decade has passed since the first prediction [1] and experimental observation [2] of ferromagnetism (FM) in transition metal (TM)-doped zinc oxide (ZnO). Nevertheless, the physical mechanisms underlying ferromagnetic order in these systems are still elusive, although in the meantime some consensus exists that ferromagnetic ordering might be intrinsic in nature and not simply related to the precipitation of metallic clusters.

Parallel to spectroscopic evidence that TMs are substituting Zn cations in the Wurtzite (WZ)-type ZnO structure [3–6], several mechanisms for the stabilization of FM were developed, involving an indirect carrier-mediated exchange mechanism [1], the percolation of polarons [7], or the presence of uncompensated spins at the surface of nanocrystals [8].

Cobalt-doped ZnO ($Zn_{1-x}Co_xO$) with a cobalt concentration $x = 0.05$–0.25 represents an archetype system for the class of TM-doped semiconductors, but, as compared to the abundance of theoretical and experimental studies on the preparation and magnetic properties, no thorough investigation of its atomic geometry has been carried out thus far. X-ray diffraction (XRD) and transmission electron microscopy (TEM) studies on $Zn_{1-x}Co_xO$ films several tens to hundreds of nanometers thick were aiming at basic information about the absence or presence of metallic precipitates and the growth of the WZ phase [9,10]. On the other hand, possible spintronic applications require controlled growth and precise knowledge of the near interface atomic geometry, since it is crucial for the device properties and for the structure of the subsequently deposited film. This has recently been demonstrated in the case of seemingly simple pure ZnO films, in which a hexagonal boron-nitride (*h*-BN) structure within the first monolayers (ML) adjacent to the Ag(111) surface was found [11].

In this Letter, we report on an *in situ* surface x-ray diffraction (SXRD) study on several monolayer-thick $Zn_{0.75}Co_{0.25}O$ films on Ag(111). The film structure is dramatically different from a random alloy commonly assumed: WZ-type CoO nanocrystals are coherently embedded within the ZnO host. The latter adopts the *h*-BN-like structure within the first layers next to the Ag(111) surface and changes to the WZ-type structure after about four layers. The experimental observations are in agreement with first-principles calculations indicating that in the ultrathin film limit CoO does not crystallize in the *h*-BN structure as ZnO does, which allows the direct identification of the two separated phases by SXRD. Our study supports the recent proposed model of a phase separation to explain the weak ferromagnetic signatures of doped ZnO films and other systems [8,12,13].

The experiments were carried out at the beam line ID32 of the European Synchrotron Radiation Facility (ESRF) in Grenoble, France. The films were deposited on Ag(111) under oxygen atmosphere ($pO_2 = 10^{-6}$ mbar) conditions by pulsed laser deposition using a KrF laser (248 nm) from a stoichiometric target (deposition rate $F = 0.017$ ML per pulse) followed by annealing up to 650 K to improve long range order. Five independent samples were prepared with a thickness between 2 and 6 ML. The sample composition was analyzed by Auger-electron spectroscopy (AES) confirming a Co concentration in the 20%–25% range.

The SXRD experiments were carried out *in situ* at a wavelength of $\lambda = 0.55$ Å under grazing incidence ($\alpha_i = 0.2°$) of the incoming beam, well above the critical angle of total reflection ($\approx 0.1°$). Figure 1 compares longitudinal scans along the b^* axis showing the first-order reflection positions of a pure ZnO- and a Co-doped film, both about 3 ML thick. The scan is indicated by the arrow in the inset. The peak positions can be determined with high precision using the first-order substrate reflection at $b^* = 1$ reciprocal lattice units (rlu) as a reference. While the peak of pure ZnO at $k = 0.875$ rlu corresponds to a 7/8 coincidence lattice on Ag(111) with a spacing of $a = b = 3.30$ Å [11], the lattice spacing of $Zn_{0.75}Co_{0.25}O$ is contracted to

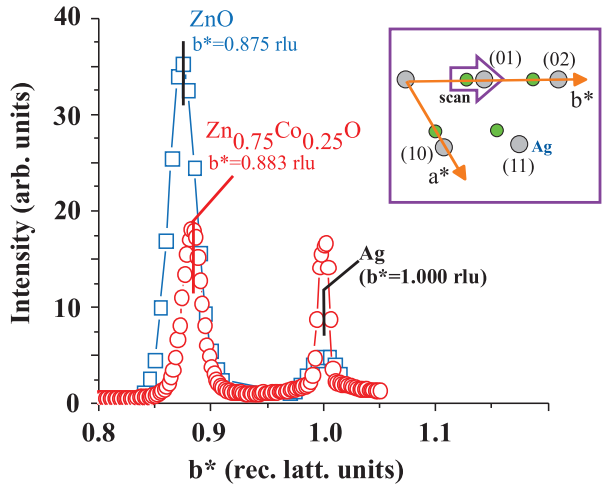

FIG. 1 (color). Scan along the b^* axis for pure ZnO (squares) and $Zn_{1-x}Co_xO$ (circles). The a^*-b^* plane in rec. space is shown in the inset. Large (gray) and small (green) circles represent rods of the Ag substrate and film, respectively. The different reflection widths originate from different instrumental resolutions.

$a = b = 3.27$ Å (peak at $k = 0.883$ rlu) due to the incorporation of the smaller Co atom into the film. There is no evidence for any asymmetric peak broadening, which allows one to rule out a large scale ($\geq$20 nm) ZnO/CoO phase separation.

The quantitative structure analysis was carried out by collecting reflection intensities along the rods up to a maximum momentum transfer of $q_z = 7$ rlu corresponding to $q_z = 6.22$ Å^{-1}. As a representative example, we discuss a 5 ML film. Symbols in Fig. 2 represent the structure factor intensities $|F(hk\ell)|^2$ along several rods (hexagonal indexing), which were derived from integrated

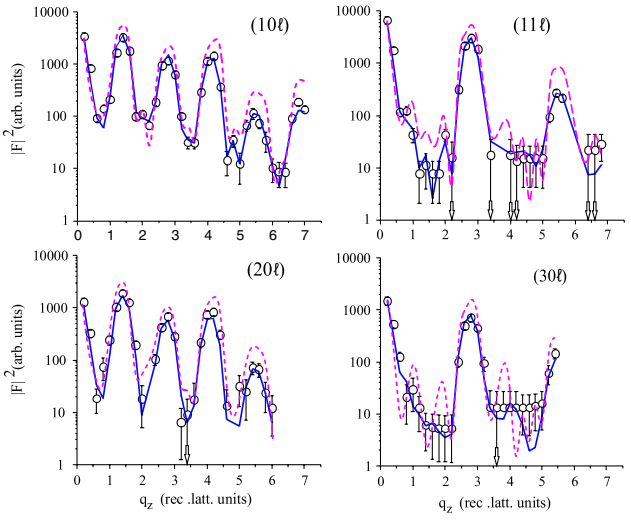

FIG. 2 (color online). Measured (symbols) and calculated (lines) structure factor intensities along rods of the 5 ML-thick doped ZnO film. Solid and dashed lines correspond to structure models with and without cation anisotropic disorder, respectively (for details see text).

intensities after correcting for geometric factors [14,15]. Error bars correspond to standard deviations derived from the counting statistics and the reproducibility of symmetry equivalent reflections, which are within the 10%–15% range. Solid lines represent the best fit using the structure model discussed below. The best fit quality is characterized by the unweighted residuum (R_u) or the goodness of fit (GOF) [16]. Excellent values of $R_u = 0.14$ and GOF = 1.27 were achieved.

Because of the high symmetry of the structure (plane group $p3m1$), only the z positions of the atoms within the unit cell need to be refined. Within each layer, oxygen and metal atoms occupy the positions $(0, 0, z)$ and $(2/3, 1/3, z + u)$ or vice versa, changing layer by layer. In the following, u is multiplied by the lattice parameter c to obtain a parameter with dimension "length" (uc). For pure ZnO it was shown recently that within the first layers uc adopts small values of $uc = 0.2 \pm 0.2$ Å. This is close to the value of the h-BN structure ($uc = 0.0$ Å) [11]. With increasing distance from the substrate, layers become WZ-like ($uc = 0.63$ Å).

The $Zn_{0.75}Co_{0.25}O$ films differ from those of pure ZnO in that the structure is characterized by a strong out of plane disorder of the atoms within the first 4–5 layers next to the substrate. As will be shown in the following, the vertical displacements are so large ($\approx$0.9 Å) that they must be attributed to static rather than to thermal disorder. In the SXRD analysis, the cation sites are identified as split into two distinct positions which are attributed to separated regions of ZnO and CoO.

A direct space image of the disorder at a given atomic site is obtained from the Fourier transformation (FT) of the atom's displacement factor $T(\vec{q})$, equivalent to the Debye-Waller damping factor in the case of harmonic thermal or static disorder ($\vec{q}$ represents the scattering vector). In the present case, a satisfactory description of the disorder requires the consideration of third-order anharmonic contributions to the Debye-Waller damping factor by using the Gram-Charlier (GC) series development: $T_{GC}(\vec{q}) = T_H(\vec{q})[1 + (1/6)(i2\pi)^3 \cdot q_k q_l q_m \cdot C^{klm}]$. Here $T_H(\vec{q}) = \exp(-8\pi^2 U^{kl} q_k q_l)$ is the harmonic (H) Debye-Waller factor containing the mean squared displacement amplitudes U^{kl} and the components q_j ($j = 1, 2, 3$) of $\vec{q}$ (for more details, see Ref. [18]).

The FT of $T_{GC}(\vec{q})$ yields the probability density function [PDF($\vec{u}$)] of the atom in real space. While in the harmonic approximation PDF($\vec{u}$) is a trivariate Gaussian function represented by an ellipsoid, anharmonic contributions account for deviations from the ellipsoidal shape. The results of the refinement [19] related to the first layer metal site, where the effect is most pronounced, are outlined in the following.

The PDF [see Fig. 3(a)] directly shows that the site is split into two distinct positions. Using the PDF maxima as a reference, the vertical separation of the peaks is about 1.3 Å. Because of the anharmonic potential and truncation

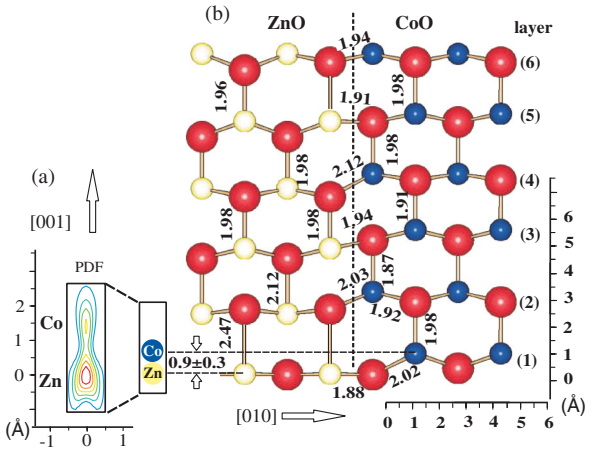

FIG. 3 (color). (a) PDF contour plot of the (Zn,Co) site in the first layer next to the Ag(111) surface. Level interval is 0.4 between 0.4 (min.) and 2.4 (max.). Maxima are related to Zn and Co. The boxes indicate the different size scale between (a) and (b). (b) Schematic structure model. WZ-type CoO is separated from *h*-BN-type ZnO. The vertical line indicates the phase boundary. Distances are given in Å, and layers are labeled from (1), next to the Ag(111) surface to (6).

errors, this value cannot directly be identified with the separation between the atoms [18]. The square root of the harmonic term ($\sqrt{U^{33}} = 0.7$ Å) represents a good estimate. This value is in reasonable agreement with the separation (0.9 ± 0.3 Å) which is found in the harmonic approximation, when the z positions of two atoms with identical (x and y) but independent z coordinates are refined. Second, the integrated peak intensity of the lower PDF peak is about 2.5 times larger than that of the upper one, consistent with the AES-derived 75:25 Zn to Co ratio. The lower and upper sites are therefore identified as occupied by Zn and Co, respectively.

Very similar PDFs are also obtained for the second and third layers, while for subsequent layers the disorder rapidly decreases approaching values of the order of magnitude of isotropic thermal disorder ($U \approx 0.01$ Å^2). Neglecting anisotropic disorder by allowing only for an overall isotropic value of $\sqrt{U^{ii}} = 0.1$ Å ($i = 1, 2, 3$), the $|F(hk\ell)|^2$ values shown as red dashed lines are calculated, strongly deviating from the experimental ones, especially at high q_z (Fig. 2).

On the basis of these results, a model can be constructed, in which the film consists of separated regions of ZnO and CoO. The basic characteristics are outlined in Fig. 3(b), which shows the structure near a CoO/ZnO interface in a projection to the *b*-*c* plane. The lowest layer labeled as (1) is next to the Ag(111) surface. Oxygen and metal atoms are represented as large and small spheres, respectively. The structure is characterized by regions of WZ-type CoO (right) coexisting with the ZnO host matrix (left). While CoO exists in the WZ-type structure with about $uc = 0.6 \pm 0.2$ Å in all layers, the ZnO phase undergoes a transition from the *h*-BN-type structure to the WZ-type structure within the first 4–5 layers next to the substrate [11]. Since in these two structure types the metal site resides at a markedly different height (Δuc) above the plane of the oxygen atoms, the vertical positions of the metal site appear as strongly disordered, because SXRD provides a space average of the structure. The oxygen atoms also exhibit disorder, although less pronounced. All distances across the interface are within 5% (0.1 Å) of the bulk values. The matching across the interface mainly involves changes of the bond angles rather than changes of the bond distances.

No quantitative information exists about size and distribution of the CoO crystals within the ZnO matrix, but a scenario of a ZnO/CoO separation with crystal sizes in the range larger than 20 nm can be ruled out by the absence of any asymmetric line broadening in the longitudinal scan (see Fig. 1). On the basis of the structure model which indicates distinct metal positions, a random alloy model (RAM) cannot be constructed. The RAM corresponds to a 25%:75% weighted "superposition" of the CoO and ZnO phases, involving nonphysically low metal-oxygen distances, many of them even below 1.5 Å.

The SXRD analysis provides several more details, some of which are shortly summarized (a thorough presentation will be published elsewhere): [20] (i) Metal-oxygen distances are within 5% of the corresponding WZ-type bulk structures (ZnO:1.98 Å, CoO:1.93 Å). Significantly larger values (2.2–2.5 Å) are observed only for the interlayer bonds in the *h*-BN-ZnO phase (see Fig. 3). (ii) Since the metal-oxygen distances are constrained to bulklike values but the uc values differ in the ZnO and the CoO domains, oxygen atoms also adopt different z positions separated by about 0.3–0.5 Å as evidenced by mean square displacement amplitude (U^{33}) values in the 0.15 Å^2 range.

An intuitive explanation for the different structural properties of ZnO and CoO was provided by Mooser and Pearson nearly 50 years ago [21] based on their concept of the "directionality" of the bonds. Since in CoO the metal-oxygen bond is more ionic than in ZnO, bulk CoO crystallizes in the sodium-chloride structure characterized by an octahedral coordination. By contrast, the less ionic ZnO crystallizes in the WZ structure with tetrahedral coordination involving more directed bonds. As shown in this study as well as in a recent low energy electron diffraction investigation [22], CoO can be stabilized in the WZ structure, but a further increase of the directionality of the bonds involved by the transition to the planar trigonal coordination in the *h*-BN structure is tolerated only by ZnO, not by CoO. This qualitative picture is confirmed quantitatively by first-principles calculations using the Vienna *Ab Initio* Simulation Package (VASP), well known for providing precise total energies and forces [23].

We first investigated the transition from the WZ to the *h*-BN structure for bulk ZnO as well as for CoO. As pointed out by Limpijumnong and Lambrecht [24], the WZ to *h*-BN transition follows a homogeneous transfor-

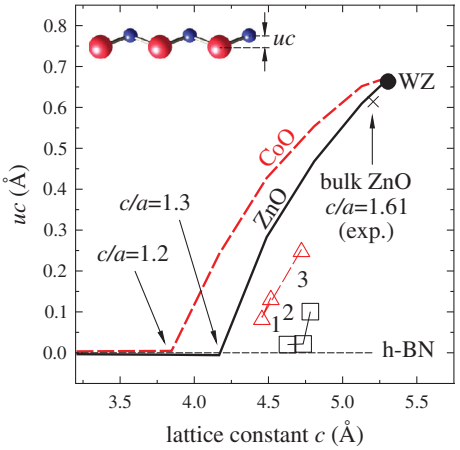

FIG. 4 (color). Calculated uc vs c for bulk ZnO and CoO (solid and dashed line, respectively). Symbols represent calculated uc values for thin films of ZnO (squares) and CoO (triangles) on Ag(111), where labels 1–3 correspond to layer numbers as in Fig. 3. Parameters uc and c for WZ, bulk ZnO, and h-BN are indicated for comparison.

mation path characterized by a decreasing c/a lattice parameter ratio. Keeping the a lattice parameter constant at $a = 3.27$ Å and allowing the uc parameter to relax, we find for ZnO that the transition takes place from $c = 5.22$ Å ($c/a = 1.61$, $uc = 0.63$ Å) to $c = 4.21$ Å ($c/a = 1.3$, $uc = 0.0$ Å) as shown by the solid (black) line in Fig. 4. Although CoO exists in the WZ phase with almost the same c lattice parameter as ZnO, the formation of the h-BN phase requires a significantly larger compression characterized by $c = 3.88$ Å ($c/a = 1.2$) directly reflecting the tendency of CoO to avoid the h-BN structure [see the dashed (red) line in Fig. 4].

Calculations were also carried out for 4 ML-thick ZnO and CoO films on Ag(111) represented by a 7 ML-thick slab. Apart from the in-plane lattice parameter $a = 3.27$ Å, all positions were relaxed using the generalized gradient approximation. Values for uc of the first three layers are shown in Fig. 4 as open squares (ZnO) and triangles (CoO), respectively. In agreement with experiment, uc is almost zero for ZnO [11,25]. For CoO we find values between 0.1 and 0.3 Å, somewhat smaller than in experiment (0.6 ± 0.2 Å) but indicating that ZnO and CoO adopt different structures (h-BN and WZ) at the interface. As compared to the bulk, the uc versus c dependencies of the films are shifted to larger values of c. We find $c = 4.4$–4.7 Å in good agreement with experiment (note that c corresponds to 2 times the spacing between layers).

Our results are important in the context of current theories explaining magnetic properties in TM-doped semiconductors in general. Recently, it was proposed that a phase separation occurs in doped ZnO and in other systems [8,12,13], in which the phase containing the magnetic impurity is coherently embedded into the nonmagnetic host. According to our first-principle simulations for all phases represented in Fig. 4, CoO is antiferromagnetic (AF) with a local magnetic moment in the 2.6–$2.8\mu_B$ range. Although it was proposed that uncompensated spins at the surface of AF CoO nanoislands might be responsible for the spontaneous magnetization in ZnCoO alloys, until now a clear-cut experimental proof for a CoO/ZnO phase separation was missing. This is due to the very similar geometric structure and electron densities of the phases involved, hardly accessible by standard XRD or TEM experiments. Our study has provided evidence that nanoassembling of CoO within the ZnO host matrix does occur supporting the phase decomposition model. It might be a more general phenomenon and should also be considered in future studies on diluted magnetic semiconductors.

We thank the ESRF staff for their hospitality in Grenoble. The help of O. Mironets during the data analysis is also acknowledged. This work is supported by the SFB 762.

[1] T. Dietl, *et al.*, Science **287**, 1019 (2000).
[2] K. Ueda, H. Tabata, and T. Kawai, Appl. Phys. Lett. **79**, 988 (2001).
[3] N. Jedrecy *et al.*, Phys. Rev. B **69**, 041308 (2004).
[4] M. Kobayashi *et al.*, Phys. Rev. B **72**, 201201 (2005).
[5] P. Sati *et al.*, Phys. Rev. Lett. **96**, 017203 (2006).
[6] A. Ney *et al.*, Phys. Rev. Lett. **100**, 157201 (2008).
[7] J. M. D. Coey, M. Venkatesan, and C. B. Fitzgerald, Nature Mater. **4**, 173 (2005).
[8] T. Dietl, *et al.*, Phys. Rev. B **76**, 155312 (2007); T. Dietl, Nature Mater. **5**, 673 (2006).
[9] H.-J. Lee *et al.*, J. Magn. Magn. Mater. **310**, 2089 (2007).
[10] M. Ivill *et al.*, New J. Phys. **10**, 065002 (2008).
[11] C. Tusche, H. L. Meyerheim, and J. Kirschner, Phys. Rev. Lett. **99**, 026102 (2007).
[12] T. Dietl, Physica (Amsterdam) **35E**, 293 (2006).
[13] S. Kuroda *et al.*, Nature Mater. **6**, 440 (2007).
[14] I. K. Robinson and D. J. Tweet, Rep. Prog. Phys. **55**, 599 (1992).
[15] E. Vlieg, J. Appl. Crystallogr. **30**, 532 (1997).
[16] R_u is defined as $R_u = \sum ||F^{\rm obs}| - |F^{\rm calc}|| / \sum |F^{\rm obs}|$, with $F^{\rm obs}$ and $F^{\rm calc}$ as observed and calculated structure factors, respectively. For GOF, see Ref. [17].
[17] R. Feindenhans'l, Surf. Sci. Rep. **10**, 105 (1989).
[18] W. F. Kuhs, Acta Crystallogr. Sect. A **48**, 80 (1992).
[19] We derived the symmetry independent parameters: $U^{11} = 0.047(11)$ Å^2, $U^{33} = 0.49(6)$ Å^2, $C^{333} = 3.6(8) \times 10^{-3}$, and $C^{113} = -0.67(19) \times 10^{-3}$.
[20] H. L. Meyerheim *et al.* (unpublished).
[21] E. Mooser and W. B. Pearson, Acta Crystallogr. **12**, 1015 (1959).
[22] W. Meyer *et al.*, Phys. Rev. Lett. **101**, 016103 (2008).
[23] G. Kresse and J. Furthmüller, Phys. Rev. B **54**, 11 169 (1996).
[24] S. Limpijumnong and W. R. L. Lambrecht, Phys. Rev. Lett. **86**, 91 (2001).
[25] C. L. Freeman *et al.*, Phys. Rev. Lett. **96**, 066102 (2006).